Fatty Acids Covalently Bound to α-Hemolysin of *Escherichia coli* Are Involved in the Molten Globule Conformation: Implication of Disordered Regions in Binding Promiscuity†

Vanesa Herlax‡ and Laura Bakás*,‡,§

Instituto de Investigaciones Bioquímicas La Plata (INIBIOLP), Facultad de Ciencias Médicas, 60 y 120 (1900) La Plata, Argentina, and Departamento de Ciencias Biológicas, Facultad de Ciencias Exactas, Universidad Nacional de La Plata, 47 y 115 (1900) La Plata, Argentina

Received August 30, 2006; Revised Manuscript Received February 16, 2007

ABSTRACT: α-Hemolysin (HlyA) is a pore-forming toxin secreted by pathogenic strains of *Escherichia coli*. The toxin is synthesized as a protoxin, ProHlyA, which is matured in the cytosol to the active form by acylation at two internal lysines, K_{563} and K_{689} (HlyA). It is widely known that the presence of fatty acids is crucial for the hemolytic and cytotoxic effects of the toxin. However, no detailed physicochemical characterization of the structural changes produced by fatty acids in the soluble protein prior to membrane binding has been carried out to date. The effects of chemical denaturants, the ANS binding parameters (K_d and n) and the sensitivity to proteases were compared between the acylated and unacylated protein forms HlyA and ProHlyA. Our results are consistent with a molten globular form of the acylated protein. Moreover, because molten globule proteins are intrinsically disordered proteins, using disorder prediction analyses, we show that HlyA contains 9 regions composed of 10−30 natively disordered amino acids. We propose that this conformation induced by covalently bound fatty acids might provide HlyA with the ability to bind to a variety of molecules during its action mechanism.

Many protein toxins from Gram-negative bacteria require activation steps to become active forms after intracellular translation. This is the case for the pore-forming α-hemolysin (HlyA[1]) of *Escherichia coli*. HlyA represents a unique class of bacterial toxins that requires a post-traslational modification involving a covalent amide linkage of fatty acids to two internal lysine residues for activation (*1*).

HlyA is a protein toxin (110 kDa) with a wide target cell specificity, and it has been associated with urinary tract infections and septicemia (*2*). It belongs to the so-called RTX (repeats in toxin) family, a series of protein toxins that contain a number of glycine- and aspartate-rich nonapeptide tandem repeats near their C-terminal end (*3*). Synthesis, maturation, and secretion of *E. coli* HlyA are determined by the *hlyCABD* operon (*4*). The gene A product is a 110-kDa polypeptide corresponding to protoxin (ProHlyA), which is matured in cytosol to the active form (HlyA) by HlyC-directed acylation. HlyA activated *in vivo* consists of a heterogeneous family of up to nine different covalent structures (two acylation sites and three possible modifying groups at each one, C 14:0 (68%), C15:0 (26%), and C17:0 (6%)) (*5*). Like other members of the family, HlyA is extracellularly secreted as a soluble protein, although an alternative secretion mechanism by outer membrane vesicles was recently identified, with both mechanisms independent of acylation (*6*) (Herlax, V., unpublished results).

In the extracellular medium, HlyA must associate with calcium in order to bind to membranes in the lytically active form (*7*, *8*). This second activation step is acylation-dependent because calcium-binding capacity is lower in the unacylated protein (*9*).

Once HlyA is activated, the toxin appears to have a two-stage interaction with membranes: reversible adsorption, sensitive to electrostatic forces, and irreversible insertion (*10*). The inserted HlyA form behaves as an integral protein because it cannot be extracted without the use of detergents (*11*). Moreover, ProHlyA, although non-acylated, also interacts with membranes. This is not surprising because the amino acid sequence of the polypeptide shows amphipathic helices in the amino acid 250−400 region. However, despite the amphipathic stretches known to be essential for lytic activity, ProHlyA is unable to alter bilayer permeability (*9*). Experiments on protein adsorption at the air−water interface suggest that the fatty acids present in HlyA but not in ProHlyA do not modify the surface-active properties of the protein and that the main difference between the precursor and the mature protein is that ProHlyA is virtually unable to insert itself into lipid monolayers (*12*). Moreover, we found that the presence of two acyl chains in HlyA confers this protein with the property of irreversible binding to

† This research is supported by the Agencia Nacional de Promoción de Ciencia y Tecnología (PICT No. 01-08645).

* To whom correspondence should be addressed. Phone: 54-221-482-4894. Fax: 54-221-4258988. E-mail: lbakas@biol.unlp.edu.ar.

‡ Instituto de Investigaciones Bioquímicas La Plata (INIBIOLP).

§ Universidad Nacional de La Plata.

[1] Abbreviations: ANS, 8-anilinonaphtalene-1-sulfonate; FRET, fluorescence resonance energy transfer; GdnHCl, guanidinium chloride; HlyA, α-Hemolysin; LB, Luria−Bertani medium; MAb, monoclonal antibody; PMSF, phenylmethylsulfonyl fluoride; ProHlyA, proHemolysin; RTX, repeats in toxin; TC, Tris-NaCl; TCU, Tris-NaCl-urea.

10.1021/bi0618013 CCC: $37.00
Published on Web 04/04/2007

membranes, which is essential for the lytic process to take place (*13*).

The increase in hydrophobicity resulting from the attachment of a fatty acid increases the association of many proteins with membranes mediating specific protein−protein and/or protein−lipid interactions, but very little is known about how acyl groups modify the protein structure in solution.

To determine if covalently bound fatty acids produce conformational changes, several methods, including chemical denaturation, ANS binding, and limited protease digestion, were employed. All these techniques are useful to unequivocally characterize the well defined different protein conformations: order, molten globule, and random coil (*14*). Our results support the hypothesis that ProHlyA presents a more compact structure, whereas HlyA has a molten globule conformation, suggesting that the fatty acids are involved in the adoption of the active protein conformation. Because the molten globule form belongs to the intrinsically disordered protein family, we discuss the importance of these intrinsically disordered regions in different steps in the action mechanism of the toxin.

MATERIALS AND METHODS

Protein purification. HlyA and ProHlyA were purified from culture filtrates of *E. coli* strains overproducing plasmids WAM 1824 (*15*) and WAM 783 (*16*), respectively (kindly provided by Dr. R. A. Welch, University of Wisconsin, Madison).

Cultures for HlyA were grown to late log phase in LB to an optical density at 600 nm (OD_{600}) of 0.8−1.0. Cells were pelleted, and the supernatant was concentrated and partially purified by precipitation with 20% cold ethanol. The precipitate containing HlyA was collected by centrifugation (1 h, 10,000 rpm in a Sorvall centrifuge, rotor SSA 34), then resuspended in 20 mM Tris at pH 7.0 and 150 mM NaCl (TC). SDS−PAGE analysis of this preparation showed a main band at 110 kDa corresponding to more than 90% of the total protein. Proteins of lower molecular mass were removed by dialysis (membrane cutoff 30 kDa). The protein was stored at −70 °C in 20 mM Tris at pH 7.0, 150 mM NaCl, and 6 M urea (TCU). Proteins were first dialyzed in TC (1:100 v/v) before each experiment, during 4 h at 4 °C.

GdnHCl Denaturation. The fluorescence emission of Trp was used to monitor HlyA denaturation at increasing concentrations of GdnHCl. Protein intrinsic fluorescence spectra were recorded on a Perkin-Elmer LS 50B spectrofluorimeter with a temperature-controlled sample holder. The excitation wavelength used was 295 nm to minimize tyrosine emission (*17*). Chemical stability was measured after incubating HlyA or ProHlyA (10 μg/mL) at various concentrations (0−5 M) of GdnHCl buffered with TC buffer at 25 °C for 2 h. After incubation, the Trp fluorescence spectra were recorded in the range 320−400 nm using 150-μL cuvettes. The ratio of the fluorescence intensity at 350 and 330 nm (X) was used to calculate f_D (molar fraction of denatured molecules) (*18*) as follows:

$$f_D = \frac{X_x - X_{\text{GdnHCl 0 M}}}{X_{\text{GdnHCl 6 M}} - X_{\text{GdnHCl 0 M}}} \qquad (1)$$

where X_x is the fluorescence intensity ratio at each GdnHCl concentration tested.

ANS Binding. The interaction of HlyA or ProHlyA with ANS was analyzed using the same spectrofluorimeter in a 150-μL fluorimetric cell at 25 °C. 1-Anilino-8-naphthalenesulfonic acid (ANS, Molecular Probes, Eugene, OR) binding curves were generated by titrating increasing amounts of protein into a fixed amount of ANS (10 μM) in TC buffer. An excitation wavelength of 350 nm was used, and fluorescence emission was recorded between 420 and 600 nm. Slits were 4 nm for both excitation and emission. ANS binding curves were measured three times for each protein and averaged.

The stoichiometry and dissociation constants (K_d) for the binding of ANS to HlyA or ProHlyA were calculated using Klotz analysis according to the methods described by Maity (*19*). Klotz graphs were necessary for the evaluation of the binding constants because nonlinear Scatchard plots were obtained for HlyA and ProHlyA.

Assuming that there are n independent binding sites for ANS per protein and the quantum yield of each site is the same, the following equation can be written as follows:

$$\frac{[P_t]}{F_{obs}/F_{max}\,[A_t]} = \frac{K_d}{n[A_t](1 - F_{obs}/F_{max})} + \frac{1}{n} \qquad (2)$$

where F_{obs} is the fluorescence intensity at a given protein concentration, and F_{max} is the maximum fluorescence when all ANS molecules are bound to protein. This calibration factor was determined to relate the change in fluorescence to the amount of ANS bound to protein. P_t is the amount of total protein added, and A_t corresponds to the concentration of ANS added. Subsequently, a fixed amount of ANS (10 μM) was titrated with increasing amounts of HlyA and ProHlyA, and from the slope and the intercept of the plot $[P_t]/(F_{obs}/F_{max})[A_t]$ versus $1/[A_t](1-F_{obs}/F_{max})$, values of K_d and n were determined.

For fluorescence resonance energy transfer (FRET) experiments, samples were excited at 295 nm to selectively excite Trp residues, and the fluorescence emission was recorded between 300 and 500 nm. The FRET efficiency was calculated from the decrease in donor fluorescence (*20*).

Limited Proteolysis. A trypsin stock solution was prepared (4 mg/mL in TC buffer), aliquoted, and frozen at −20 °C until used. Proteolysis experiments contained HlyA or ProHlyA/trypsin at a 5:1 molar ratio in TC buffer at pH 7.4. They were allowed to react for 0.5, 1, 5, 15, and 30 min at room temperature. The reaction was stopped by the addition of 0.1 mM PMSF, and the digests were analyzed by 10% SDS−PAGE. The intensity of the main band was analyzed using Kodak Digital Science 1D Software.

Computational Analyses. ProHlyA was analyzed for regions of putatively disordered structure using neural network-based predictions (PONDR, *Predictor of Naturally Disordered Regions*, available at www.pondr.com). The length-dependent predictor of intrinsic protein disorder algorithm, VSL1, developed by Peng and Obradovic was used. We chose this predictor because it is the most accurate and gives the best results of the 20 order/disorder predictors tested (*21*).

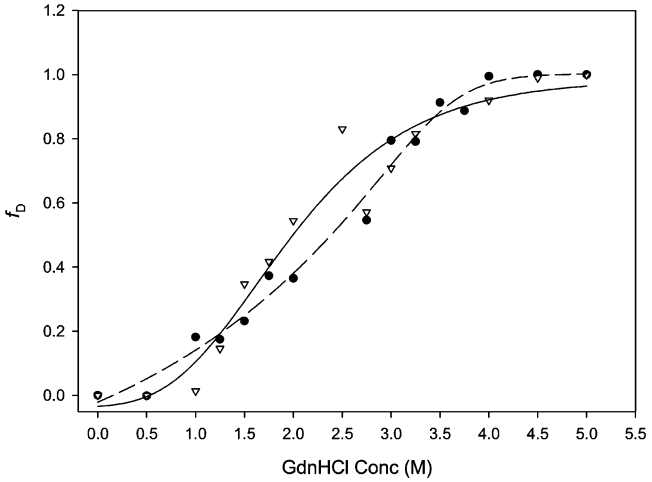

FIGURE 1: Chemical denaturation of HlyA (▽) and ProHlyA (●) at different GdnHCl concentrations in TC buffer at pH 7.4 and 25 °C quantified from the ratio between fluorescence intensity at 350 and 330 nm (*X*). f_D (molar fraction of denatured molecules) was estimated as $f_D = (X_x - X_{GdnHCl\ 0\ M})/(X_{GdnHCl\ 6\ M} - X_{GdnHCl\ 0\ M})$, where X_x is the fluorescence intensity ratio at each GdnHCl concentration tested. The excitation wavelength was 295 nm. Data were fitted to sigmoidal curves using the curve-fitting procedures in SigmaPlot (Jandel Scientific, San Rafael, CA). The continuous and dashed lines correspond to HlyA and ProHlyA denaturation curves, respectively. The protein concentration was 10 μg/mL.

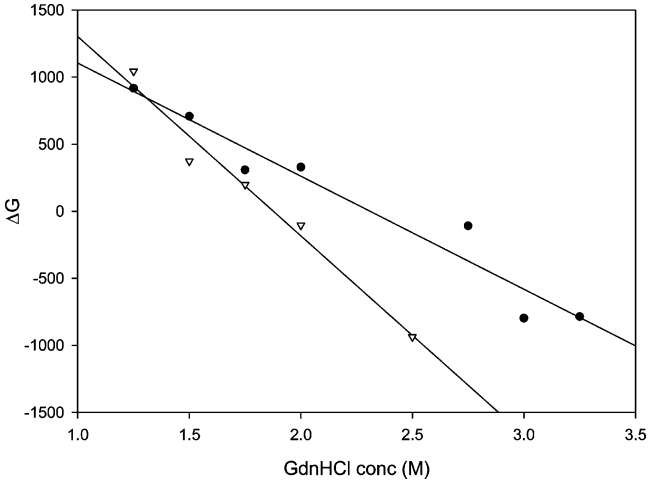

FIGURE 2: Dependence of the unfolding free energy ($\Delta G°$) with denaturant concentration for HlyA (▽) and ProHlyA (●). *m* and $\Delta G°_{H_20}$ were calculated from the slope and ordinate intercept, respectively.

RESULTS

GdnHCl Denaturation. Denaturing curves are suitable for measuring differences in conformational stability among proteins. The relative concentration of folded (native) and unfolded conformations can be determined from studies in which spectral probes are used to monitor the conformational state of the protein (*22*). HlyA is a 1023 amino acid protein containing 4 tryptophan (W) residues located at positions 431, 479, 578, and 913, which can serve as intrinsic fluorophores. The ratio between the relative fluorescence intensity at 350 and 330 nm increases because of the red shift of W fluorescence upon denaturation, indicating a more polar environment for W residues in the unfolded state. From this ratio, it was possible to estimate f_D (mole fraction of denatured molecules) (Figure 1).

GdnHCl unfolding transitions reached a plateau, and a two-model state fits the experimental data. The GdnHCl concentration required to reach the midpoint of the transition between both states (C_m) was higher for ProHlyA in comparison with that for acylated HlyA. The unfolding curves for both ProHlyA and HlyA are not abrupt, probably reflecting the existence of local differences in the unfolding of different regions tested by W-residue fluorescence.

Because the unfolding event consists of an equilibrium process involving two states, it allows for the definition of the equilibrium constant $K = f_D/(1-f_D)$. Hence, the Gibb's free energy for the unfolding reaction in terms of these mole fractions at a particular GdnHCl concentration ($\Delta G° = -RT \ln K$) can be calculated. The dependence of $\Delta G°$ on GdnHCl concentration can be approximated by the linear equation $\Delta G° = \Delta G°_{H_2O} - m$[GdnHCl], where the free energy of unfolding in the absence of denaturant ($\Delta G°_{H_2O}$), which represents the conformational stability of the protein, can be obtained by extrapolating to zero denaturant concentration. *m* is a coefficient that is proportional to the amount of hydrophobic regions of the protein that are exposed to solvent when the protein unfolds (*23*). C_m, GdnHCl concentration at the midpoint of the denaturating transition, can be obtained at $\Delta G° = 0$. As observed in Figure 2, $\Delta G°_{H_2O}$, *m*, and C_m show acylation dependence.

ANS Binding. To confirm the more relaxed structure of HlyA, ANS binding behavior was evaluated. ANS is a probe for monitoring hydrophobic areas in protein molecules. It is almost nonfluorescent in aqueous medium, but the quantum yield increases significantly after binding to hydrophobic sites on a protein surface. For this reason, it is a suitable probe for quantitative evaluation of the average surface hydrophobicity of a protein in its native state (*24*). The binding of ANS to both HlyA and ProHlyA is associated with enhanced fluorescence and a blue shift in ANS emission wavelength (data not shown). K_d and *n* were calculated as described in Materials and Methods. First, a plot of $1/\Delta F$ versus 1/[protein] was extrapolated to infinite protein concentration to calculate F_{max} values of 3.7 and 3.34 AU/μM ANS bound for HlyA and ProHlyA, respectively. These values indicate that the fluorescence increase per ANS bound to protein is similar in both cases, suggesting a similar environment for the probe. From Figure 3, the values calculated for *n* are 19.6 and 38.5, and the K_d values are 1.6 and 16.6 μM for ProHlyA and HlyA, respectively. K_d values determined in this way are only apparent values because an uncertain number of ANS molecules can bind with possibly different quantum yields.

Resonance energy transfer between the W residues of proteins and ANS molecules has been reported (*20*). The fluorescence emission maximum for ProHlyA in solution is blue-shifted in comparison to that of HlyA, suggesting that the W residues are located in a more hydrophobic environment in the unacylated protein, as we previously reported (*13*). The emission was quenched by the addition of ANS, and a second emission peak at 470 nm appeared corresponding to an ANS−protein complex, indicating the transference of energy from W to adsorbed ANS molecules. In the absence of ANS, maximum fluorescence was emitted at 347 nm because of W excitation; with increasing ANS concentration, this emission decreased, and the emission intensity of ANS increased (data not shown). As observed

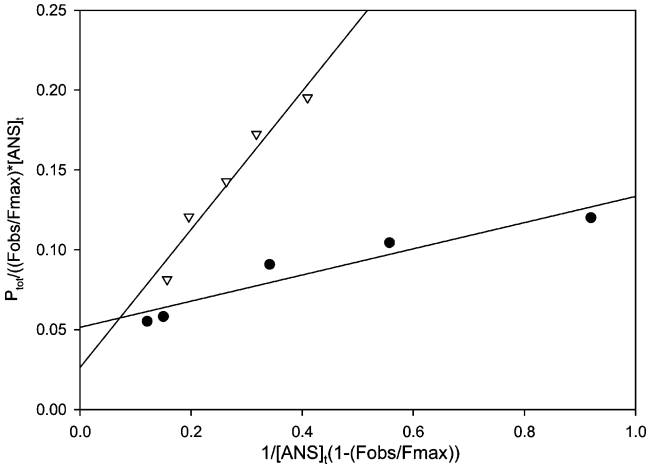

FIGURE 3: Plot of $P_{tot}/((F_{obs}/F_{max}) \times [ANS]t)$ vs $1/[ANS]t(1 - (F_{obs}/F_{max}))$ for the complex ANS−Hly (▽) and complex ANS−ProHlyA (●) to determine K_d and n from the slope and intercept, respectively. ANS binding curves were generated by titrating increasing amounts of protein into a fixed amount of ANS (10 μM) in an appropriate buffer. An excitation wavelength of 350 nm was used, and fluorescence emission was recorded between 420 and 600 nm.

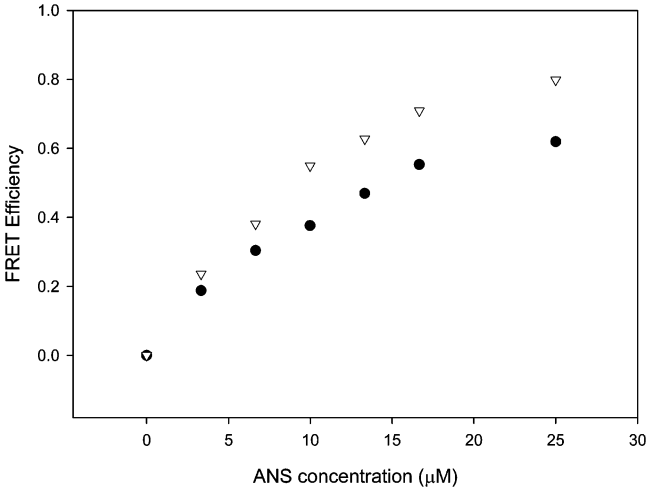

FIGURE 4: FRET efficiency determination from Trp to ANS for 10 μg/mL HlyA (▽) and ProHlyA (●) using ANS concentrations of 0−20 μM. The excitation wavelength was 295 nm, and FRET efficiency was calculated from the decrease in donor fluorescence at 350 nm.

in Figure 4, the energy transfer efficiency calculated from the decrease in donor fluorescence was higher for HlyA than for ProHlyA. It is possible to estimate binding constants from the Trp−ANS energy transfer process; the apparent dissociation constants for ANS were similar to those determined by ANS fluorescence for HlyA and ProHlyA (data not shown).

Limited Proteolysis. Limited protease degradation of proteins is useful in determining the compactness or flexibility in regions of folded proteins by observing their resistance to digestion (*25*). Furthermore, unstructured or partially structured proteins can be characterized by their sensitivity to protease digestion (*26*). To experimentally test for the presence of disordered regions in HlyA and ProHlyA, we utilized limited proteolysis to determine if the presence of the acyl chain in HlyA increases the rate of digestion. As described in Materials and Methods, both HlyA and ProHlyA were digested with trypsin. The reaction was stopped at different times, and samples were analyzed by SDS−PAGE. HlyA disappeared after the first minute (Figure 5A), whereas the unacylated protein was digested more slowly, in accordance with its more compact conformation (Figure 5B). Figure 5C shows the intensity of the main band versus time for both HlyA and ProHlyA.

Computational Analyses. Because molten globule proteins are intrinsically disordered proteins, HlyA was further analyzed for the presence of putatively disordered regions. Recently, a number of groups have published predictors of protein disorder, several of which are available on the web, as reviewed by Uversky et al. (*27*). These predictors are based on the assumption that the absence of a rigid structure is encoded by specific features of the amino acid sequence. In fact, statistical analysis shows that amino acid sequences encoding for intrinsically disordered (ID) proteins or regions are significantly different from those of ordered proteins on the basis of local amino acid composition, flexibility, hydrophobicity, charge, coordination number, and several other factors.

We used a recently developed disorder prediction algorithm (PONDR-VSL1) to determine the potential of ProHlyA to achieve these dynamic flexible structures. The sequence was analyzed and is illustrated in Figure 6. The amino acid sequence is represented on the *x*-axis, and the prediction of disorder is on the *y*-axis. Peaks >0.5 are strongly predicted to be disordered.

Prediction results show that ProHlyA contains disordered regions, located mainly from the middle to the C-terminal end of the protein. The regions composed of at least 8 aa are 377−385, 508−523, 528−543, 553−561, 678−693, 748−779, 827−839, 1002−1013, and 1015−1023. Thus, fatty acids covalently bound to the protein can potentially expose some disordered regions. The functional significance of these regions is discussed below.

DISCUSSION

The ability of HlyA to bind to a variety of molecules is consistent with the concept that the binding sites of this toxin must be dynamic, and the protein possibly lacks a rigid tertiary structure.

Our results show that HlyA has a molten globule conformation promoted by the presence of acyl chains, as demonstrated by a lower denaturing GdnHCl concentration. Thus, a higher number of ANS molecules bind to HlyA with weak affinity, and there is higher efficiency of energy transfer from W to ANS and a faster digestion with trypsin compared to that with ProHlyA.

Molten globule proteins typically unfold at low concentrations of denaturant and do not show a sigmoidal unfolding curve, thus indicating a lack of cooperativity (*28*), although for HlyA a slight degree of cooperativity was observed (Figure 1). The event becomes somewhat complicated in proteins containing mixtures of ordered and molten globular regions because the ordered part is expected to unfold cooperatively at higher denaturant concentrations, whereas the molten globular part unfolds with little or no cooperativity at lower denaturant concentrations (*29*). As observed in Figure 2, $\Delta G°_{H_2O}$ and m showed acylation dependence. The acylated protein was more stable in the absence of denaturant than the unacylated form, as demonstrated by a higher

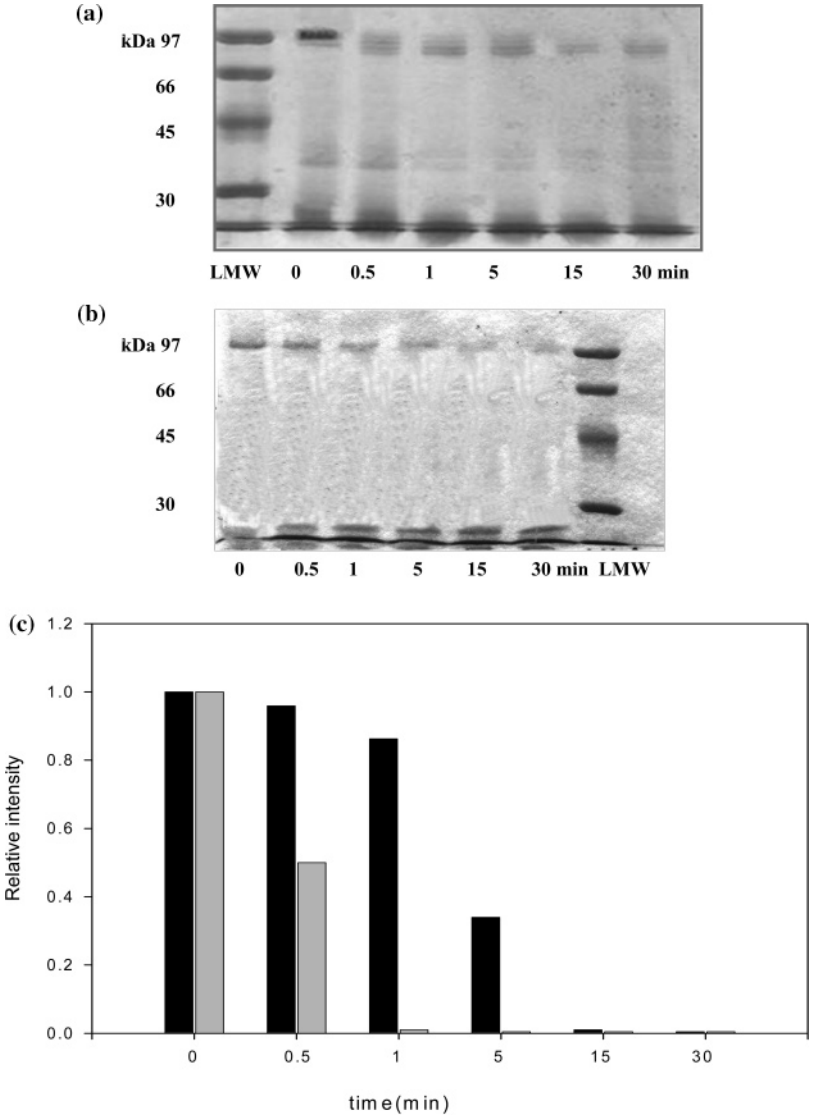

FIGURE 5: Digestion products of HlyA (A) and ProHlyA (B) analyzed by 10% SDS−PAGE stained with Coomassie Blue. Proteolysis experiments contained HlyA or ProHlyA/trypsin at a 5:1 molar ratio in TC buffer at pH 7.4. They were allowed to react for 0.5, 1, 5, 15, and 30 min at room temperature. The reaction was stopped by the addition of 0.1 mM PMSF. LMW: low molecular weight markers. The relative intensity of the band corresponding to HlyA (black bars) and ProHlyA (gray bars) measured using Kodak Science software was plotted as a function of time (C).

$\Delta G°_{H_2O}$ value, 2.4 and 1.4 kcal/mol for HlyA and ProHlyA, respectively. However, acyl chains covalently bound to the protein promote steric hindrance that contributes to a more relaxed structure, which can thus be denatured at a lower GdnHCl concentration. HlyA unfolds at 1.9 M, whereas ProHlyA unfolds at 2.3 M GdnHCl.

$\Delta G°$ decreases more rapidly with increasing denaturant concentration for HlyA, as expected because of the greater hydrophobic surface exposed during denaturation according to the higher *m* value obtained: 803.93 and 418.4 cal/mol M for HlyA and ProHlyA, respectively.

As mentioned above, ANS binding to ordered regions can be distinguished from the binding to molten globule-like regions by differences in the apparent binding constant. The exceptionally high value of *n* found for HlyA and ProHlyA (Figure 3) might be due to amphipathic regions in both forms, but it can be observed that the presence of fatty acids doubles the *n* value due to the molten structure they impart. Although the high number of ANS molecules bound is unusual, the same behavior was found for bacteriorhodopsin ($n = 50$), which has an appreciable degree of surface hydrophobicity consistent with the location of this protein *in vivo*, embedded in the nonpolar environment of the purple bacteria membrane (*24*). The binding of a large number of ANS molecules in a weak manner, as demonstrated by the K_d values, is characteristic of the loose structure of the molten conformation. Operationally, ANS binding to pockets in ordered or molten globule proteins gives apparent K_d values that differ by more than a factor of 5; thus, despite the uncertainties, these apparent K_d values serve as a diagnostic tool to distinguish ordered from molten proteins (*30*). This difference is also observed between HlyA and ProHlyA K_d values, demonstrating once again that fatty acids induce a molten structure. Moreover, the higher fluorescence transfer efficiency for HlyA compared to that for ProHlyA indicates that the quenching of W fluorescence was more effective when the binding of ANS to the molten globule conformation takes place, where the accessibility of both surface and inner W residues is increased. Thus, the capability of ANS to quench Trp fluorescence is correlated with ANS binding behavior.

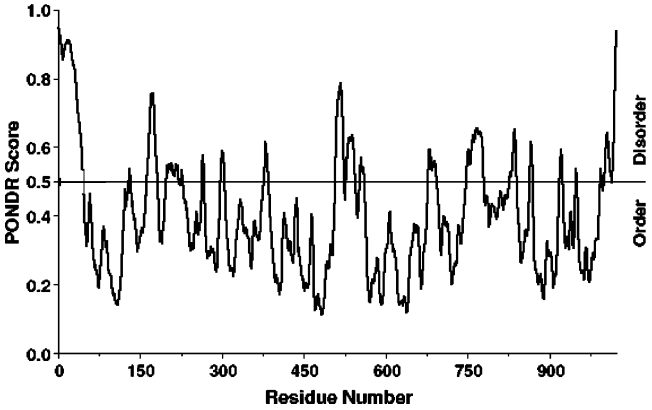

FIGURE 6: Prediction of disordered regions of ProHlyA analyzed by the predictor of natively disorder regions, PONDR. The amino acid sequence is represented on the *x*-axis, and the prediction of disorder is on the *y*-axis. Peaks >0.5 are strongly predicted to be disordered.

As mentioned above, proteins with molten globule-like regions are included in the category of intrinsically disordered proteins, as recently reviewed elsewhere (*31*).

As shown in Figure 6, most of the disordered regions of ProHlyA predicted using PONDR are located in the C-terminal half of the protein, which could be related to different steps of the action mechanism of this toxin involving its recognition for extracellular transport to pore formation in target cells.

HlyA carries a carboxy-terminal secretion signal located within the last 50−60 aa (*32*). A poorly defined secondary or tertiary structure at the carboxy-terminus is needed for HlyB-, HlyD-, and TolC-mediated export (*33*). This region is predicted to be disordered, and although it was observed that export of the toxin is acylation-independent (*34*), the extracellular transport yield was lower for ProHlyA compared to that for HlyA. In addition, a high concentration of ProHlyA was found in inclusion bodies (*12*), and thus, covalently bound acyl chains can also expose these regions and facilitate transport.

Intrinsically unstructured proteins can bind in several different patterns in a process termed binding promiscuity. The intrinsic lack of structure can confer functional advantages, including the ability to bind, perhaps in different conformations, to several different target cells, explaining the ambiguity in experimental determinations of the presence of a receptor for HlyA published to date (*35*−*37*).

Many studies have searched for the presence of a receptor for HlyA in different target cells. For example, CD11a and CD18, the two subunits of $\beta 2$ integrin, were identified as cell-surface receptors that mediate HlyA toxicity in human target cells HL60 (*35*). This receptor was found in most circulating leukocytes (lymphocytes, neutrophils, monocytes, and macrophages). Despite the absence of studies identifying the protein region responsible for the interaction with this receptor, studies of adenylate cyclase−hemolysin of *Bordetella pertusis* (CyaA), another RTX toxin, revealed that the main integrin-interacting domain of CyaA is located in its glycine/aspartate-rich repeat region, which is characteristic of all protein members of this family (*38*). These results allowed the identification of region 1166−1287 as a major CD11b-binding motif (*39*). Because this domain is involved in calcium binding, the authors proposed that CyaA shifts from a disordered structure to an α-helical conformation upon calcium binding to the RTX motifs (*40*); therefore, it is tempting to speculate that the Ca^{2+}-binding domain composed of glycine-rich tandem repeats corresponding to aa 550−850 of HlyA might be involved in the binding to β_2 integrin. It is important to note that these regions also match with the disordered regions predicted and that acyl chains might be implicated in the exposure because the Ca^{2+}-binding capacity of ProHlyA is lower than that of HlyA (*9*).

Another protein identified as a receptor of HlyA in horse erythrocytes is the glycoprotein glycophorin (*36*). A glycophorin-binding region between residues 914 and 936 was identified (*41*). Previous sequence analyses of several RTX toxins revealed that this is a conserved region. If this region is deleted, the specific binding of HlyA to the cell-surface receptors on erythrocytes is lost without affecting the nonspecific binding (adsorption) to lipid bilayers. As shown in Figure 6, this region is also predicted to be intrinsically disordered.

Recently, studies carried out with staphylococcal α-toxin showed that the high susceptibility of rabbit erythrocytes to the pore-forming action of this toxin correlates with the presence of saturable, high-affinity binding sites. Evidence was presented that phosphocholine head groups of sphingomyelin, clustered in sphingomyelin−cholesterol microdomains, serve as receptors for α-toxin, a process required for oligomerization (*42*). A binding site for phospholipid headgroups is located in a cleft lined by W179 and R200 residues in staphylococcal α-toxin. A similar situation was reported for leukocidin Luk (*43*). Similarly, residues W913 and R935 are found in HlyA, and they are also present in the predicted disordered region. This can probably explain the high susceptibility of rabbit erythrocytes (*44*), cells that lack glycophorin in their membranes that can act as a receptor for HlyA (*45*).

It is known that lipid binding to proteins is also a determinant of specific protein−protein interactions such as the assembly of proteins into oligomeric complexes. This is the case for HlyA, where an oligomer was found at lytic concentrations in ghosts of sheep erythrocytes. In contrast, no oligomer structure was found for ProHlyA (Herlax, V., et al., unpublished results). In addition, an important role of acylation in the oligomerization process to form hemolytic pores was proposed for CyaA (*46*).

The importance of fatty acids in the exposure of disordered regions is supported by results published for D12 mAb epitope reactivity. The D12 epitope maps to aa 673−726. The D12 mAb reacts with HlyA, but not with ProHlyA; therefore, acylation is directly responsible for the exposition of the epitope within this region (*47*, *48*).

Finally, if we take into account that the acylation of internal lysine residues and the presence of intrinsic disorder regions are rare in prokaryotic proteins, then both events should be important in the action mechanism of this toxin.

ACKNOWLEDGMENT

L.S.B. is a member of Carrera del Investigador CIC-PBA, Argentina. V.H. is a fellow of CONICET, Argentina.

REFERENCES

1. Stanley, P., Koronakis, V., and Hughes, C. (1998) Acylation of *Escherichia coli* hemolysin: a unique protein lipidation mecha-

nism underlying toxin function, *Microbiol. Mol. Biol. Rev. 62*, 309−333.
2. Cavalieri, S., Boach, G., and Snyder, I. (1984) *Escherichia coli* alpha-hemolysin: characteristics and probable role in pathogenicity, *Microbiol. Rev. 4*, 326−333.
3. Cotte, J. G. (1992) Structural and functional relationships among the RTX toxin determinants of Gram negative bacteria, *FEMS Microbiol. Rev. 88*, 137−162.
4. Welch, R. A. (2001) RTX toxin structure and function: a story of numerous anomalies and few analogies in toxin biology, *Curr. Top. Microbiol. Immunol. 257*, 85−111.
5. Lim, K. B., Bazemore Walker, C. R., Guo, L., Pellett, S., Shabanowitz, J., Hunt, D., Hewlett, E. L., Ludwig, A., Goebeli, W., Welch, R. A., and Hackett, M. (2000) *Escherichia coli* α-Hemolysin (HlyA) is heterogeneously acylated in vivo with 14-, 15-, and 17-carbon fatty acids, *J. Biol. Chem. 275*, 36698−36702.
6. Balsalobre, C., Silvan, J. M., Berglund, S., Mizunoe, Y., Uhlin, B. E., and Wai, S. N. (2006) Release of the type I secreted alpha-haemolysin via outer membrane vesicles from *Escherichia coli*, *Mol. Microbiol. 59*, 99−112.
7. Ostolaza, H., Soloaga, A., and Goñi, F. M. (1995) The binding of divalent cations to *Escherichia coli* alpha-haemolysin, *Eur. J. Biochem. 228*, 39−44.
8. Bakás, L., Veiga, M., Soloaga, A., Ostolaza, H., and Goñi, F. (1998) Calcium-dependent conformation of *E. coli* alpha-haemolysin. Implications for the mechanism of membrane insertion and lysis, *Biochim. Biophys. Acta 1368*, 225−234.
9. Soloaga, A., Ostolaza, H., Goñi, F. M., and de la Cruz, F. (1996) Purification of *Escherichia coli* pro-haemolysin, and a comparison with the properties of mature alpha-haemolysin, *Eur. J. Biochem. 238*, 418−422.
10. Bakás, L., Ostolaza, H., Vaz, W. L., and Goñi, F. M. (1996) Reversible adsorption and nonreversible insertion of *Escherichia coli* alpha-hemolysin into lipid bilayers, *Biophys. J. 71*, 1869−1876.
11. Soloaga, A., Veiga, M. P., García-Segura, L., Ostolaza, H., Brasseur, R., and Goñi, F. M. (1999) Insertion of *Escherichia coli* a-haemolysin in lipid bilayers as a non-transmembrane integral protein: prediction and experiment, *Mol. Microbiol. 31*, 1013−1024.
12. Sanchez-Magrañer, L., Cortajarena, A., Goni, F. M., and Ostolaza, H. (2006) Membrane insertion of *Escherichia coli* alpha-hemolysin is independent from membrane lysis, *J. Biol. Chem 281*, 5461−5467.
13. Herlax, V., and Bakás, L. (2003) Acyl chains are responsible for the irreversibility in the *Escherichia coli* α-hemolysin binding to membrane, *Chem. Phys. Lipids 122*, 185−190.
14. Uversky, V. (2002) Natively unfolded proteins: A point where biology waits for physics, *Protein Sci. 11*, 739−756.
15. Moayeri, M., and Welch, R. A. (1997) Prelytic and lytic conformations of erythrocyte-associated *Escherichia coli* hemolysin, *Infect. Immun. 65*, 2233−2239.
16. Boehm, D., Welch, R., and Snyder, I. (1990) Domains of *Escherichia coli* hemolysin (HlyA) involved in binding of calcium and erythrocyte membranes, *Infect. Immunol. 58*, 1959−1964.
17. Valpuesta, J., Goñi, F., and Macarulla, J. (1987) Tryptophan fluorescence of mitochondrial complex III reconstituted in phosphatidylcholine bilayers, *Arch. Biochem. Biophys. 257*, 285−292.
18. Lackowicz, J. (1984) *Principles of Fluorescence Spectroscopy*, Plenum Press, New York.
19. Maity, H., and Kasturi, S. (1998) Interaction of bis (1-anilino-8-napthalenesulfonte) with yeast hexoquinase: a steady-state fluorescence study, *J. Photochem. Photobiol., B 47*, 190−196.
20. Long-Sen, C., Her-Ya, W., Jen-Jung, H., and Chung-Chang, C. (1994) Energy transfer from tryptophan residues of proteins to 8-anilinonaphtalene-1-sulfonate, *J. Protein Chem. 13*, 635−640.
21. Dunker, A. K., Cortese, M. S., Romero, P., Iakoucheva, L. M., and Uversky, V. (2005) Flexible nets. The roles of intrinsic disorder in protein interaction networks, *FEBS J. 272*, 5129−5148.
22. Pace, C. (1986) Determination and analysis of urea and guanidine hydrochloride denaturation curves, *Methods Enzymol. 131*, 266−280.
23. Myers, J., Pace, C., and Scholtz, J. (1995) Denaturant m values and heat capacity changes: relation to changes in accessible surface areas of protein unfolding, *Protein Sci. 4*, 2138−2148.
24. Cardamone, M., and Puri, N. K. (1992) Spectrofluorimetric assessment of the surface hydrophobicity of proteins, *Biochem. J. 282*, 589−593.
25. Creighton, T. E. (1984) *Proteins, Stuctures and Molecular Properties*, 1st ed., W. H. Freeman and Co., New York.
26. Kriwacki, R. W., Wu, J., Tennant, L., Wright, P. E., and Siuzdak, G. (1997) Probing protein structure using biochemical and biophysical methods. Proteolysis, matrix-assisted laser desorption/ionization mass spectrometry, high-performance liquid chromatography and size-exclusion chromatography of p21Waf1/Cip1/Sdi1, *J. Chromatogr., A 777*, 23−30.
27. Uversky, V. N., Oldfield, C. J., and Dunker, A. K. (2005) Showing your ID: intrinsic disorder as an ID for recognition, regulation and cell signaling, *J. Mol. Recognit. 18*, 343−384.
28. Chamberlain, A. K., and Marqusee, S. (1998) Molten globule unfolding monitored by hydrogen exchange in urea, *Biochemistry 37*, 1736−1742.
29. Jamin, M., Antalik, M., Loh, S. N., Bolen, D. W., and Baldwin, R. L. (2000) The unfolding enthalpy of the pH 4 molten globule of apomyoglobin measured by isothermal titration calorimetry, *Protein Sci. 9*, 1340−1346.
30. Bailey, R. W., Dunker, A. K., Brown, C. J., Garner, E. C., and Griswold, M. D. (2001) Clusterin, a binding protein with a molten globule-like region, *Biochemistry 40*, 11828−11840.
31. Dunker, K., Lawson, J. D., Brown, R. M., Williams, P., and Romero, J. S. (2001) Intrinsically disordered protein, *J. Mol. Graphics Modell. 19*, 26−59.
32. Jarchau, T., Chakraborty, T., Garcia, F., and Goebel, W. (1994) Selection for transport competence of C-terminal polypeptides derived from *Escherichia coli* hemolysin: the shortest peptide capable of autonomous HlyB/HlyD-dependent secretion comprises the C-terminal 62 amino acids of HlyA, *Mol. Gen. Genet. 245*, 53−60.
33. Forestier, C., and Welch, R. A. (1991) Identification of RTX toxin target cell specificity domains by use of hybrid genes, *Infect. Immun. 59*, 4212−4220.
34. Ludwig, A., Vogel, M., and Goebel, W. (1987) Mutations affecting activity and transport of haemolysin in *Escherichia coli*, *Mol. Gen. Genet. 206*, 238−254.
35. Lally, E. T., Kieba, I. R., Sato, A., Green, C. L., Rosenbloom, J., Korostoff, J., Wang, J. F., Shenker, B. J., Ortlepp, S., Robinson, M. K., and Billings, P. C. (1997) RTX toxins recognize a beta2 integrin on the surface of human target cells, *J. Biol. Chem. 272*, 30463−30469.
36. Cortajarena, A., Goñi, F. M., and Ostolaza, H. (2001) Glycophorin as a receptor for *Escherichia coli* α-hemolysin in erythrocytes, *J. Biol. Chem. 276*, 12513−12519.
37. Valeva, A., Walev, I., Kemmer, H., Weis, S., Siegel, I., Boukhallouk, F., Wassenaar, T., Chavakis, T., and Bhakdi, S. (2005) Binding of *Escherichia coli* hemolysin and activation of the target cells is not receptor-dependent, *J. Biol. Chem. 280*, 36657−36663.
38. Azami-El-Idrissi, M. E., Bauche, C., Loucka, J., Osicka, R., Sebo, P., Ladant, D., and Leclerc, C. (2003) Interaction of *Bordetella pertussis* adenylate cyclase with CD11b/CD18: role of toxin acylation and identification of the main integrin interaction domain, *J. Biol. Chem 278*, 38514−38521.
39. Guermonprez, P., Khelef, N., Blouin, E., Rieu, P., Ricciardi-Castagnoli, P., Guiso, N., Ladant, D., and Leclerc, C. (2001) The adenylate cyclase toxin of *Bordetella pertussis* binds to target cells via the Mβ2 integrin (CD11b/CD18), *J. Exp. Med. 193*, 1035−1041.
40. Rose, T., Sebo, P., Bellalou, J., and Ladant, D. (1995) Interaction Of calcium with *Bordetella Pertussis* adenylate cyclase toxin characterization of multiple calcium-binding sites and calcium-induced conformational changes, *J. Biol. Chem. 270*, 26370−26376.
41. Cortajarena, A. L., Goñi, F. M., and Ostolaza, H. (2003) A receptor- binding region in *Escherichia coli* α-haemolysin, *J. Biol. Chem 278*, 19159−19163.
42. Valeva, A., Hellmann, N., Walev, I., Strand, D., Plate, M., Boukhallouk, F., Hanada, K., Decker, H., and Bhakdi, S. (2006) Evidence that clustered phosphocholine head groups serve as sites for binding and assembly of an oligomeric protein pore, *J. Biol. Chem. 281*, 26014−26021.
43. Kaneko, J., and Kamio, Y. (2004) Bacterial two-component and hetero-heptameric pore-forming cytolytic toxins: structures, pore-forming mechanism and organization of the genes, *Biosci. Biotechnol. Biochem. 68*, 981−1003.
44. Rennie, R. P., and Arbuthnott, J. P. (1974) Partial characterization of *Escherichia coli* haemolysin, *J. Med. Microbiol. 7*, 179−188.

45. Ligi, F., Ciacci, C., Palma, F., and Palma, F. (1998) Comparative study of the cytoplasmic domain of band 3 from human and rabbit erythrocyte membranes, *Comp. Biochem. Physiol., B 121*, 265−271.
46. Hackett, M., Walker, C., Guo, L., Gray, M. C., Cuyk, S. V., Ullmann, U., Shabanowitz, J., Hunt, D. F., Hewlett, E. L., and Sebo, P. (1995) Hemolytic, but not cell-invasive activity of adenylate cyclase toxin is selectively affected by differential fatty-acylation in *Escherichia coli*, *J. Biol. Chem. 270*, 20250−20253.
47. Pellett, S. D., Boehm, F., Snyder, I. S., Rowe, G., and Welch, R. A. (1990) Characterization of monoclonal antibodies against the *Escherichia coli* hemolysin, *Infect. Immun. 58*, 822−827.
48. Rowe, G. E., Pellett, S., and Welch, R. A. (1994) Analysis of toxinogenic functions associated with the RTX repeat region and monoclonal antibody D12 epitope of *Escherichia coli* hemolysin, *Infect. Immun.* 62, 579−588.

BI0618013